= $\sigma(F_o^2)/2F_o$ and $\sigma(F_o^2) = [\sigma^2(I) + (AI)^2]^{1/2}/Lp$, the fudge factor *A* being assumed equal to 0.03.

The final values of the conventional *R* and $R_w$ agreement indices were 0.042 and 0.053, respectively.

The final difference-Fourier map showed some residual peaks of up to ca. 1.5 e Å$^{-3}$, close to the rhenium atoms, which prevented a direct location of the hydridic atoms. Fourier maps, computed at decreasing values of $(\sin\theta)/\lambda$, did not show peaks suitable for these atoms. They were placed in idealized positions but not included in the structure factor calculations. The locations were calculated by determining the intersection point of the two (CO)–Re vectors trans to each hydride. This led to two different situations: the hydrides bridging the long Re–Re edges and almost lying in the Re$_3$ plane (Hy(1) and Hy(2)) gave mean Re–H and Re–H–Re bond parameters of 1.70 Å and 140°, while the hydrides bridging the short metal–metal bond (Hy(3) and Hy(4)) gave corresponding mean values of 1.94 Å and 92°. We have then moved the hydrides along the lines defined by these calculated points and the centers of the subtended Re–Re edges, ca. 0.30 Å outward in the first case (up to mean Re–H and Re–H–Re parameters of 1.82 Å and 122°) and slightly inward (ca. 0.12 Å) in the second case (up to mean Re–H and Re–H–Re parameters of 1.86 Å and 97°). The final bond parameters result quite similar to analogous interactions determined by neutron diffraction studies.[3,6a,23]

The final positional parameters are reported in Table II.

**Acknowledgment.** We thank the Italian CNR for financial support.

**Registry No.** 1, 64478-51-9; [ReH$_2$(CO)$_4$](NEt$_4$), 67047-76-1; [Re$_3$($\mu$-H)$_3$(CO)$_{13}$](NEt$_4$)$_2$, 60544-31-2; [Re$_3$($\mu$-H)$_2$(CO)$_{12}$](NEt$_4$), 96791-00-3; [Re$_3$($\mu$-H)$_2$(CO)$_{12}$]$^-$, 51779-06-7; [Re$_3$($\mu$-H)$_4$(CO)$_{10}$](PPN), 96760-23-5; Re$_3$($\mu$-H)$_3$(CO)$_{12}$, 73463-62-4.

**Supplementary Material Available:** Tables of thermal parameters, calculated positions for the hydrogen atoms, and observed and calculated structure factors (34 pages). Ordering information is given on any current masthead page.

---

Contribution from the Division of Applied Organic Chemistry, CSIRO, Melbourne, Victoria 3001, Australia,
and Research School of Chemistry, The Australian National University, Canberra, ACT 2601, Australia

# Energy Transfer vs. Electron Transfer in the Excited-State Quenching of Tris(2,2′-bipyridine-*N*,*N*′)ruthenium(II) Complexes by Cobalt(III) Cage Complexes: Applications to the Photoreduction of Water

INGE I. CREASER,[1a] LAWRENCE R. GAHAN,[1a] RODNEY J. GEUE,[1a] ANTON LAUNIKONIS,[1b]
PETER A. LAY,[1b] JOHN D. LYDON,[1a] MARK G. McCARTHY,[1a] ALBERT W.-H. MAU,*[1b]
ALAN M. SARGESON,*[1a] and WOLFGANG H. F. SASSE*[1b]

*Received December 21, 1984*

A variety of cobalt cage complexes act as electron-transfer agents (ETA) in the [Ru(bpy)$_3$]$^{2+}$/ETA/Pt(PVA)/edta-mediated photoreduction of water (bpy = 2,2′-bipyridine; Pt(PVA) = colloidal platinum dispersion on polyvinyl alcohol; edta = 1,2-ethanediamine-*N*,*N*,*N*′,*N*′-tetraacetic acid). At pH 5.0 a very narrow potential range of the Co(III)/Co(II) couple (∼−0.25 to −0.42 V vs. NHE) is suitable for acceptably efficient ($0.05 \lesssim \Phi(^1/_2\mathrm{H_2}) \lesssim 0.10$) photoreduction of water. The most effective cage complex is [Co(CLsar)]$^{3+}$ (CLsar = 1-chlorosar = 1-chloro-3,6,10,13,16,19-hexaazabicyclo[6.6.6]eicosane). At $4 \times 10^{-3}$ M, methylviologen (mv$^{2+}$) and [Co(CLsar)]$^{3+}$ are comparable in their abilities to produce hydrogen, while at $2 \times 10^{-3}$ M, mv$^{2+}$ is about 3 times as efficient. The narrow bell-shaped potential vs. rate of H$_2$ production curve obtained is due to the lack of thermodynamic driving force for water reduction at more positive potentials and an increased competition of energy-transfer over electron-transfer quenching of [Ru*(bpy)$_3$]$^{2+}$ at more negative potentials. With [Ru(4,4′-Me$_2$bpy)$_3$]$^{2+}$ as sensitizer, the curve is displaced to more negative potentials in concert with the greater reducing power of its excited state compared with that of [Ru*(bpy)$_3$]$^{2+}$. The quenching constants observed for the cage complexes reacting with the Ru(II) excited states are generally lower than those of viologen molecules of the same electrochemical potential. This partially explains the increased concentrations of cage complexes required to obtain maximum rates of H$_2$ production. The sulfur-containing capten cobalt cage complexes (capten = 1-methyl-6,13,19-triaza-3,10,16-trithiabicyclo[6.6.6]eicosane) and sar cage complexes with potentials ≳−0.2 V vs. NHE are very efficient oxidative quenching agents for [Ru*(bpy)$_3$]$^{2+}$ with quenching rate constants approaching those of mv$^{2+}$ and quantum yields approaching unity. Thus solvent-cage escape before back electron transfer is not considered a limiting factor to oxidative quenching by cage complexes in contrast to the case for viologens. Although the reduction potentials of these complexes are too high (∼0 V vs. NHE) at pH 5.0 for reduction of water, at pH ∼0 quantum yields for H$_2$ production approach unity. Cage complexes based on sar with neutral substituents become more effective quenching agents of the excited states of the ruthenium sensitizers as the Co(III)/Co(II) redox potential is made more positive. Those with potentials more positive than −0.34 V vs. NHE quench [Ru*(bpy)$_3$]$^{2+}$ exclusively (≳95%) by electron transfer; however, their ability to produce hydrogen at pH 5.0 is limited by zero to unfavorable free energy changes. By contrast, electron transfer contributes less than 50% to the quenching of [Ru*(4,4′-Me$_2$bpy)$_3$]$^{2+}$ by cage complexes. The major advantage of the cage complexes is their long-term stability in the photochemical cycles compared to that of viologens.

## Introduction

There are now available a large variety of encapsulated cage complexes of Co(III),[2–14] which are substitution inert in both the Co(III) and Co(II) oxidation states.[2,4–8,10–15] The kinetic inertness of the Co(II) states is unusual, and it allows the Co(II)/Co(III) oxidation states to be cycled without loss of complex integrity.

---

(1) (a) The Australian National University. (b) CSIRO.

(2) Sargeson, A. M. *Pure Appl. Chem.* **1978**, *50*, 905; *Chem. Br.* **1979**, *15*, 23; *ACS Symp. Ser.* **1980**, *No. 119*, 115.

(3) Harrowfield, J. M.; Herlt, A. J.; Sargeson, A. M. *Inorg. Synth.* **1980**, *20*, 85.

(4) Creaser, I. I.; Harrowfield, J. M.; Herlt, A. J.; Sargeson, A. M.; Springborg, J.; Geue, R. J.; Snow, M. R. *J. Am. Chem. Soc.* **1977**, *99*, 3181. Creaser, I. I.; Geue, R. J.; Harrowfield, J. M.; Herlt, A. J.; Sargeson, A. M.; Snow, M. R.; Springborg, J. *Ibid.* **1982**, *104*, 6016.

(5) Geue, R. J.; Hambley, T. W.; Harrowfield, J. M.; Sargeson, A. M.; Snow, M. R. *J. Am. Chem. Soc.* **1984**, *106*, 5478.

(6) Hammershøi, A.; Sargeson, A. M. *Inorg. Chem.* **1983**, *22*, 3554.

(7) Gahan, L. R.; Hambley, T. W.; Sargeson, A. M.; Snow, M. R. *Inorg. Chem.* **1982**, *21*, 2699.

(8) Geue, R. J.; McCarthy, M. G.; Sargeson, A. M. *J. Am. Chem. Soc.* **1984**, *106*, 8282.

(9) Geue, R. J.; McCarthy, M. G.; Sargeson, A. M.; Skelton, B. W.; White, A. H. *Inorg. Chem.* **1985**, *24*, 1607.

(10) Gainsford, G. J.; Geue, R. J.; Sargeson, A. M. *J. Chem. Soc., Chem. Commun.* **1982**, 233.

(11) Petri, W.; Sargeson, A. M.; Snow, M. R., to be submitted for publication.

(12) Gahan, L. R.; Sargeson, A. M. *Aust. J. Chem.* **1981**, *34*, 2499.

(13) Lay, P. A.; Sargeson, A. M., to be submitted for publication in *Inorg. Chem.*

(14) Lay, P. A. Ph.D. Thesis, The Australian National University, 1981.

(15) Bond, A. M.; Lawrance, G. A.; Lay, P. A.; Sargeson, A. M. *Inorg. Chem.* **1983**, *22*, 2010.

0020-1669/85/1324-2671$01.50/0

It also facilitates detailed analysis of the thermodynamics and kinetics of their electron-transfer properties.[2,4,6,8,11-25] Some cage complexes have been found to be effective electron-transfer agents (ETA) in the photochemical reduction of water,[26-28] while energy transfer predominates with others.[26] Therefore, it is clear that cobalt cage complexes possess desirable properties for use as ETA's, including the following: (i) very high stability in the Co(III) and Co(II) oxidation states; (ii) photochemical inertness to solar radiation in both oxidation states; (iii) ready control of redox potential of the Co(III)/Co(II) couple in the region useful for Scheme I by changing apical ligand substituents; (iv) the ability to change the rate of electron self-exchange of the Co(III)/Co(II) couple by alteration of the structure of the cage ligand (Table VIII); (v) the ability to control the charge of the complexes by the introduction of charged substituents and hence alter electrostatic work terms; (vi) the ability to alter steric factors that may affect quenching.

**Scheme I**

$$[\mathrm{Ru(bpy)_3}]^{2+} + h\nu \rightarrow [\mathrm{Ru^*(bpy)_3}]^{2+}$$

$$[\mathrm{Ru^*(bpy)_3}]^{2+} \xrightarrow{k_1} [\mathrm{Ru(bpy)_3}]^{2+} \quad (1)$$

$$[\mathrm{Ru^*(bpy)_3}]^{2+} + \mathrm{ETA} \xrightarrow{k_2} [\mathrm{Ru(bpy)_3}]^{3+} + \mathrm{ETA^-} \quad (2)$$

$$[\mathrm{Ru^*(bpy)_3}]^{2+} + \mathrm{ETA} \xrightarrow{k_{2'}} [\mathrm{Ru(bpy)_3}]^{2+} + \mathrm{ETA^*} \quad (2')$$

$$[\mathrm{Ru(bpy)_3}]^{3+} + \mathrm{ETA^-} \xrightarrow{k_3} [\mathrm{Ru(bpy)_3}]^{2+} + \mathrm{ETA} \quad (3)$$

$$2\mathrm{ETA^-} + 2\mathrm{H^+} \xrightleftharpoons{k_4,\ \mathrm{Pt(PVA)}} 2\mathrm{ETA} + \mathrm{H_2} \quad (4)$$

$$[\mathrm{Ru(bpy)_3}]^{3+} + \mathrm{edta} \rightarrow [\mathrm{Ru(bpy_3)}]^{2+} + \mathrm{edta^{+\cdot}} \quad (5)$$

$$\mathrm{edta^{+\cdot}} \rightarrow \text{products} \quad (6)$$

$$\mathrm{ETA} = \text{Co(III) cages or viologens}$$

These factors are now examined to provide insights into improving hydrogen-producing cycles such as those shown in Scheme I, by the use of the cage complexes. The sar (I)[26] and sep (II)[26-28] cage complexes were shown to be effective ETA's for the production of hydrogen, while the oxosar (III) and capten (IV) cage complexes were not.[26,29] In this paper, we have extended our work,[26] to include detailed studies on the pH dependencies of rates of $H_2$ production, quenching rate constants, quantum yields, and redox potentials of these complexes and the related absar (V) and the 1,2-cyclohexanediamine-based (char) (VI) cage complexes,[29] in systems using tris(2,2′-bipyridine-*N*,*N*′)ruthenium(II), $[\mathrm{Ru(bpy)_3}]^{2+}$, as a sensitizer in the sacrificial system shown in Scheme I. Equation 2′ is an energy-transfer pathway that at present we cannot distinguish from the back-reaction of $\mathrm{Ru^{III}{\cdot}ETA^-}$ within the solvent cage. Equation 3 is the back-reaction for solvent-separated Ru(III) + $\mathrm{ETA^-}$. These systems are compared with the well-studied[30-53] systems that utilize viologens as ETA's.

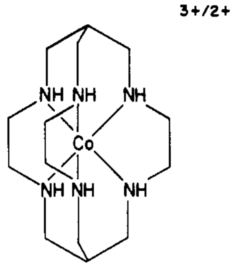

I

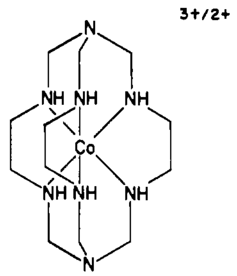

II

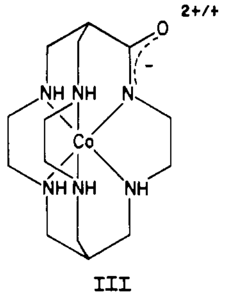

III

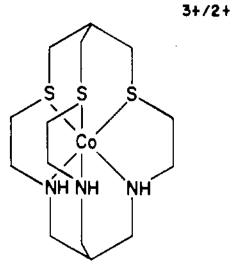

IV

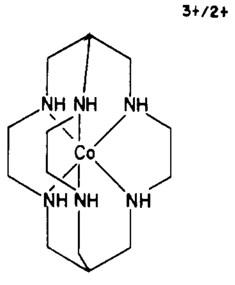

V

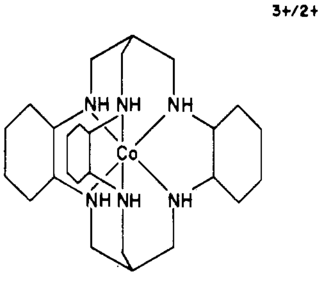

VI

---

(16) Lawrance, G. A.; Lay, P. A.; Sargeson, A. M., to be submitted for publication in *J. Am. Chem. Soc.*

(17) Lay, P. A.; Sargeson, A. M., to be submitted for publication in *J. Am. Chem. Soc.*

(18) Lay, P. A.; Hupp, J. T.; Sargeson, A. M.; Weaver, M. J., to be submitted for publication in *Inorg. Chem.*

(19) Hupp, J. T.; Lay, P. A.; Liu, H.-Y.; Petri, W.; Sargeson, A. M.; Weaver, M. J. *J. Electroanal. Chem. Interfacial Electrochem.* **1984**, *163*, 371.

(20) Creaser, I. I.; Sargeson, A. M.; Zanella, A. W. *Inorg. Chem.* **1983**, *22*, 4022.

(21) Bakac, A.; Espensen, J. H.; Creaser, I. I.; Sargeson, A. M. *J. Am. Chem. Soc.* **1983**, *105*, 7624.

(22) Dubs, R. V.; Gahan, L. R.; Sargeson, A. M. *Inorg. Chem.* **1983**, *22*, 2523.

(23) Hammershøi, A.; Lawrance, G. A.; Sargeson, A. M., to be submitted for publication in *Inorg. Chem.*

(24) Gahan, L. R.; Lawrance, G. A.; Sargeson, A. M. *Inorg. Chem.* **1984**, *23*, 4369.

(25) Lydon, J. D.; Geue, R. J.; McCarthy, M. G., unpublished results.

(26) Lay, P. A.; Mau, A. W.-H.; Sasse, W. H. F.; Creaser, I. I.; Gahan, L. R.; Sargeson, A. M. *Inorg. Chem.* **1983**, *22*, 2347.

(27) Houlding, V.; Geiger, T.; Kölle, V.; Grätzel, M. *J. Chem. Soc., Chem. Commun.* **1982**, 681.

(28) Scandola, M. A. R.; Scandola, F.; Indelli, A.; Balzani, V. *Inorg. Chim. Acta* **1983**, *76*, L67.

(29) The trivial nomenclature used for the cage complexes has been described in detail elsewhere.[15] The CM substituent is chloromethyl: sar = 3,6,10,13,16,19-hexaazabicyclo[6.6.6]eicosane; sep = 1,3,6,8,10,13,16,19-octaazabicyclo[6.6.6]eicosane; oxosar = 2-oxo-3,6,10,13,16,19-hexaazabicyclo[6.6.6]eicosane; capten = 1-methyl-6,13,19-triaza-3,10,16-trithiabicyclo[6.6.6]eicosane; absar = 3,6,10,13,15,18-hexaazabicyclo[6.6.5]nonadecane; char = 3,10,14,21,24,31-hexaazapentacyclo[10.10.10.$0^{4,9}$.$0^{15,20}$.$0^{25,30}$]dotriacontane; bpy = 2,2′-bipyridine; 4,4′-$\mathrm{Me_2}$bpy = 4,4′-dimethyl-2,2′-bipyridine.

(30) Moradpour, A.; Amouyal, E.; Keller, P.; Kagan, H. *Nouv. J. Chim.* **1978**, *2*, 547.

(31) Krasna, A. I. *Photochem. Photobiol.* **1980**, *31*, 75.

(32) Kiwi, J.; Grätzel, M. *J. Am. Chem. Soc.* **1979**, *101*, 7214.

(33) Kiwi, J.; Grätzel, M. *Nature (London)* **1979**, *281*, 657.

(34) Adams, M. W. W.; Rao, K. K.; Hall, D. O. *Photobiochem. Photobiophys.* **1979**, *1*, 33.

(35) Gohn, M.; Getoff, N. *Z. Naturforsch., A* **1979**, *34A*, 1135.

(36) Keller, P.; Moradpour, A.; Amouyal, E.; Kagan, H. B. *Nouv. J. Chim.* **1980**, *4*, 377.

(37) Keller, P.; Moradpour, A.; Amouyal, E.; Kagan, H. *J. Mol. Catal.* **1980**, *7*, 539.

(38) Balzani, V.; Moggi, L.; Manfrin, M. F.; Bolletta, F.; Gleria, M. *Science (Washington, D.C.)* **1975**, *189*, 852.

(39) Schumacher, E. *Chimia* **1978**, *32*, 193.

(40) Bolton, J. R. *Science (Washington, D.C.)* **1978**, *202*, 705.

(41) Koryakin, B. V.; Dzhabiev, T. S.; Shilov, A. E. *Dokl. Phys. Chem. (Engl. Transl.)* **1977**, *233*, 620.

(42) Kirch, M.; Lehn, J.-M.; Sauvage, J.-P. *Helv. Chim. Acta* **1979**, *62*, 1345.

(43) DeLaive, P. J.; Sullivan, B. P.; Meyer, T. J.; Whitten, D. G. *J. Am. Chem. Soc.* **1979**, *101*, 4007.

(44) Okura, I.; Kim-Thuan, N. *Chem. Lett.* **1980**, 1511.

(45) Kalyanasundaram, K.; Kiwi, J.; Grätzel, M. *Helv. Chim. Acta* **1978**, *61*, 2720.

(46) Harriman, A.; Porter, G. Richoux, M.-C. *J. Chem. Soc., Faraday Trans. 2* **1981**, *77*, 1939.

**Table I.** Quenching of $[Ru^*(bpy)_3]^{2+}$ by Co(III) Cage Complexes at 20 °C[q]

| electron-transfer agent | $E°$, V $(NaClO_4)^{a,b}$ | $E°$, $V^{a,c}$ | $10^{-8}k_q{}^d$, $M^{-1}\ s^{-1}$ | $\Phi_{max}{}^e$ | $\Phi(Co(II))^f$ | $10^{-8}k_2{}^g$, $M^{-1}\ s^{-1}$ | $10^{-8}k_{2'}{}^h$, $M^{-1}\ s^{-1}$ | $k_2/k_q{}^i$ |
|---|---|---|---|---|---|---|---|---|
| $[Co(HYMEoxosar\text{-}H)]^{2+}$ | −0.59 | −0.63 | 0.7 (2.8) | 0.08 | $<10^{-4}$ | $<10^{-3}$ | 0.7 | <0.001 |
| $[Co(CMMEabsar)]^{3+}$ | −0.51 | −0.59 | 0.7 (1.5) | 0.08 | $\lesssim 10^{-4}$ | $\lesssim 10^{-3}$ | 0.7 | ≲0.001 |
| $[Co(EFMEoxosar\text{-}H)]^{2+}$ | −0.51 | −0.58 | 1.0 (3.6) | 0.11 | $\lesssim 10^{-4}$ | $\lesssim 10^{-3}$ | 1.0 | ≲0.001 |
| $[Co(sar)]^{3+}$ | −0.40 | −0.46 | 0.16 (2.2) | 0.020 | 0.0004 | 0.032 | 0.13 | 0.2 |
| $[Co(AZAMEsar)]^{3+}$ | −0.34 | −0.43 | 0.45 | $0.05_5$ | 0.017 | 0.14 | 0.31 | 0.3 |
| $[Co(AMMEsar)]^{3+}$ | $-0.35^j$<br>$-0.18^k$ | −0.36 | 0.6 (3.3) | 0.06 | 0.01 | 0.1 | 0.5 | 0.2 |
| *lel*$_3$-$[Co(diAZAchar)]^{3+}$ | $-0.40^l$ | −0.40 | 1.4 (4.2) | 0.15 | 0.027 | 0.25 | 1.1 | 0.18 |
| $[Co(Clsar)]^{3+}$ | −0.26 | −0.36 | 1.4 (3.0) | 0.15 | 0.052 | 0.49 | 0.9 | 0.35 |
| $[Co(sep)]^{3+}$ | −0.26 | −0.35 | 1.5 (5.5)<br>$2.2,^m\ 3.6^n$ | 0.16 | 0.040 | 0.38 | 1.1 | 0.25 |
| $[Co(MENOsar)]^{3+}$ | −0.19 | −0.29 | 2.1 | 0.21 | 0.056 | 0.56 | 1.5 | $0.27^p$ |
| $[Co(CLHOsar)]^{3+}$ | −0.16 | −0.28 | 2.0 (7.6) | 0.20 | 0.19 | 1.9 | 0.1 | 0.95 |
| $[Co(diCLsar)]^{3+}$ | −0.13 | −0.25 | 2.2 (9.6) | 0.22 | 0.24 | 2.2 | $<10^{-2}$ | 1 |
| $[Co(diAMsar)]^{3+}$ | $-0.30^j$<br>$+0.06^k$ | −0.21 | 0.44 | $0.05_3$ | 0.033 | 0.27 | 0.17 | 0.62 |
| *lel*$_3$-$[Co(diAMchar)]^{3+}$ | $-0.35^j$<br>$0.00^{k,l}$ | −0.26 | 0.8 (4.0) | $0.09_3$ | 0.040 | 0.32 | 0.5 | 0.43 |
| $[Co(CLNOsar)]^{3+}$ | −0.06 | −0.17 | 4.5 | 0.37 | 0.41 | 4.5 | $<10^{-2}$ | 1 |
| $[Co(diNOsar)]^{3+}$ | +0.04 | −0.07 | 6.1 | 0.44 | 0.40 | 5.6 | ≲0.5 | 0.91 |
| $[Co(AZAcapten)]^{3+}$ | −0.01 | −0.02 | 13.2 (58) | 0.62 | 0.6 | $12._8$ | 0.4 | $0.9_7$ |
| $[Co(AMcapten)]^{3+}$ | $+0.06^k$ | +0.01 | 11.0 (180) | 0.58 | 0.31 | 5.9 | 6 | 0.53 |
| $methylviologen^{2+}$ | −0.44 | −0.44 | 9.6 | 0.54 | $0.10^o$ | 9.6 | | |
| $benzylviologen^{2+}$ | −0.36 | −0.36 | 14 | 0.64 | $0.17^o$ | 14 | | |

[a] vs. NHE. [b] Values obtained from ref 14 and 15. [c] Redox potential measured under photolysis conditions, i.e. $10^{-2}$ M edta, $HOAc/OAc^-$ buffer (pH 5.0, $\mu = 0.2$ M). [d] Obtained from linear Stern–Volmer plots. Values in parentheses are for 0.5 M $NaClO_4$. [e] Maximum possible electron-transfer quenching at $2 \times 10^{-3}$ M in complex, calculated from the quenching constants by $\Phi_{max} = k_q[Co(III)]/(k_q[Co(III)] + k_1)$. $k_1 = 1.6 \times 10^6\ s^{-1}$ under the conditions. [f] Observed Co(II) quantum yield at $2 \times 10^{-3}$ M in complex. Allowances were made for Co(II) absorbance. [g] Calculated rate constants for electron-transfer quenching $k_2 = k_q\Phi(Co(II))/\Phi_{max}$. [h] $k_{2'} = k_q - k_2$. [i] Ratio of electron-transfer pathway as compared to electron and energy transfer. [j] Redox potential of the complex in which the amine substituents are not protonated. [k] Redox potential of the complex in which the amine substituents are protonated. [l] $\mu = 0.1$ M $NaCF_3SO_3$.[8,25] [m] 0.1 M NaCl.[27] [n] 1 M $H_2SO_4$.[28] [o] Yield of $mv^{+}\cdot$ or $bz^{+}\cdot$.[51] This value is less than $\Phi_{max}$ because of low cage-escape yield. The value is dependent on experimental conditions. [p] This value may be lower than the actual value due to reduction of the nitro group by Co(II). [q] $\mu = 0.1$ M $NaClO_4$ unless otherwise stated.

We have also examined the sensitizer tris(4,4′-dimethyl-2,2′-bipyridine-*N*,*N*′)ruthenium(II), $[Ru(4,4'\text{-}Me_2bpy)_3]^{2+}$, in order to probe the effect of changing excited-state reduction potential on the competition between energy transfer and electron transfer.

## Experimental Section

The preparation and characterization of all cage complexes has been described elsewhere.[2-14,25,54] The Pt(PVA) catalyst[50,55] and $[Ru(bpy)_3]Cl_2\cdot 6H_2O$[56] were prepared by standard techniques. The 4,4′-$Me_2$bpy ligand was prepared by a modification of the procedure used for bpy.[57]

$[Ru(4,4'\text{-}Me_2bpy)_3](ClO_4)_2\cdot 3H_2O$ was synthesized by reaction of $RuCl_3\cdot 3H_2O$ (3.8 mmol, 1 g) with 4,4′-$Me_2$bpy (10.9 mmol, 2 g) in DMF (50 mL) under reflux for 60 h. The DMF was removed, and the residue was dissolved in the minimum of aqueous EtOH (1:4). After precipitation with concentrated $NaClO_4$, the solid was recrystallized from aqueous EtOH (1:4). After further purification by chromatography on Sephadex LH-20 with methanol as eluant, the major component was collected and recrystallized as before. Anal. Calcd for $C_{36}H_{36}Cl_2N_6O_8\cdot 3H_2O$: C, 47.69; H, 4.67; Cl, 7.82; N, 9.27; O, 19.4. Found: C, 47.75; H, 4.50; Cl, 7.8; N, 9.48; O, 19.1. *Caution*! *Perchlorate salts of ruthenium complexes are potentially explosive.*

Methylviologen (Aldrich), $Na_2edta$, $NaOAc\cdot 3H_2O$, AcOH, $Na_2HPO_4$, and $NaH_2PO_4$ were all AR grade chemicals and were used without further purification. Experiments were generally performed in acetate buffer (pH 5.0, 18.9 g/L $NaOAc\cdot 3H_2O$ + 3.6 g/L AcOH); otherwise, standard acetate and phosphate buffers were utilized.[58]

Electrochemical measurements were performed as described previously[15] in 0.01 M $Na_2edta$, acetate buffer (pH 5.0) solutions. All redox potentials were measured with use of both cyclic voltammetry and dc polarography, and values are quoted against the normal hydrogen electrode (NHE). Instrumentation and conditions for laser flash photolyses[52] and continuous-flow photolysis experiments[49,52] are as previously described. For experiments involving low concentrations of Pt, the cells are freshly cleaned with aqua regia prior to photolysis experiments, as small amounts of Pt(PVA) adhering to the walls of the vessel resulted in higher yields of $H_2$ than from freshly cleaned cells. Quenching constants were obtained from linear Stern–Volmer plots of lifetime measurements.

Transient quantum yields for Ru(III) production were determined by comparing the reduction of the $[Fe(OH_2)_6]^{3+}$ ion ($2 \times 10^{-2}$ M) with $[Ru^*(bpy)_3]^{2+}$ by the method described.[59,60] Quantum yields for Co(II) production were examined by following the decay in absorbance of the Co(III) complexes at their maxima[4,5,7,8,9,11,25] in continuous-radiation experiments. Corrections were made for extinction coefficients of Co(II) complexes (~10% that of Co(III)) at the wavelength used for determining Co(III) concentration and for absorption of Co(III) complexes at the excitation wavelengths (460 or 405 nm).

To determine the stability of the cage complexes under photolysis conditions, and hence extrapolated turnover numbers as defined by Lehn et al.,[42] the reaction mixtures were examined by HPLC[49] immediately before and after the photolysis. An aqueous solution of THF (10%), acetic acid (1%), sodium heptanesulfonate monohydrate (0.08%), and methanesulfonic acid (0.02%) neutralized to pH 3.1 with tetramethylammonium hydroxide was used as eluant. Large-scale photolyses (1 g

---

(47) Frank, A. J.; Stevenson, K. L. *J. Chem. Soc., Chem. Commun.* **1981**, 593.
(48) Miller, D.; McLendon, G. *Inorg. Chem.* **1981**, *20*, 950.
(49) Johansen, O.; Launikonis, A.; Loder, J. W.; Mau, A. W.-H.; Sasse, W. H. F.; Swift, J. D.; Wells, D. *Aust. J. Chem.* **1981**, *34*, 981.
(50) Johansen, O.; Launikonis, A.; Loder, J. W.; Mau, A. W.-H.; Sasse, W. H. F.; Swift, J. D.; Wells, D. *Aust. J. Chem.* **1981**, *34*, 2347.
(51) Launikonis, A.; Loder, J. W.; Mau, A. W.-H.; Sasse, W. H. F.; Wells, D. *Isr. J. Chem.* **1982**, *22*, 158.
(52) Launikonis, A.; Loder, J. W.; Mau, A. W.-H.; Sasse, W. H. F.; Summers, L. A.; Wells, D. *Aust. J. Chem.* **1982**, *35*, 1341.
(53) Kalyanasundaram, K. *Coord. Chem. Rev.* **1982**, *46*, 159.
(54) Harrowfield, J. M.; Herlt, A. J.; Lay, P. A.; Sargeson, A. M.; Bond, A. M.; Mulac, W. A.; Sullivan, J. C. *J. Am. Chem. Soc.* **1983**, *105*, 5503.
(55) Rampino, L. D.; Nord, F. F. *J. Am. Chem. Soc.* **1941**, *63*, 2745.
(56) Broomhead, J.; Young, C. G. *Inorg. Synth.* **1982**, *21*, 127 and references therein.
(57) Sasse, W. H. F. *Org. Synth.* **1966**, *46*, 5; *J. Chem. Soc.* **1959**, 3046. Sasse, W. H. F.; Whittle, C. P. *J. Chem. Soc.* **1961**, 1347.
(58) Perrin, D. D.; Dempsey, B. "Buffers for pH and Metal Ion Control"; Chapman and Hall: London, 1974.
(59) Lin, C.-T.; Sutin, N. *J. Phys. Chem.* **1976**, *80*, 97.
(60) Taylor, D. G.; Demas, J. N. *J. Chem. Phys.* **1979**, *71*, 1032.

**Table II.** Quenching of $[Ru^*(4,4'\text{-}Me_2bpy)_3]^{2+}$ by Co(III) Cage Complexes at 20 °C[a]

| electron-transfer agent | $10^{-8}k_q$, $M^{-1}\ s^{-1}$ | $\Phi_{max}$[b] | $\Phi$(Co(II))[c] | $10^{-8}k_2$, $M^{-1}\ s^{-1}$ | $10^{-8}k_{2'}$, $M^{-1}\ s^{-1}$[d] | $k_2/k_q$[d] |
|---|---|---|---|---|---|---|
| $[Co(CMMEabsar)]^{3+}$ | 0.5 | $0.03_3$ | $\lesssim 10^{-4}$ | $\lesssim 10^{-3}$ | 0.5 | $\lesssim 0.003$ |
| $[Co(EFMEoxosar\text{-}H)]^{2+}$ | 0.7 | $0.04_7$ | $\lesssim 10^{-4}$ | $\lesssim 10^{-3}$ | 0.7 | $\lesssim 0.002$ |
| $[Co(sar)]^{3+}$ | 0.59 | $0.04_0$ | $0.002_2$ | 0.033 | 0.56 | 0.056 |
| $[Co(AZAMEsar)]^{3+}$ | 0.90 | $0.05_9$ | $0.008_3$ | 0.12 | 0.78 | 0.14 |
| $[Co(AMMEsar)]^{3+}$ | 0.80 | $0.05_3$ | $0.005_3$ | 0.080 | 0.72 | 0.10 |
| *lel*$_3$-$[Co(diAZAchar)]^{3+}$ | 2.5 | $0.15_6$ | 0.017 | 0.27 | 2.2 | 0.11 |
| $[Co(CLsar)]^{3+}$ | 2.4 | 0.14 | 0.035 | 0.68 | 1.7 | 0.25 |
| $[Co(sep)]^{3+}$ | 2.4 | 0.14 | 0.014 | 0.24 | 2.2 | 0.10 |
| $[Co(MENOsar)]^{3+}$ | 3.8 | 0.21 | 0.004[f] | ... | ... | ... |
| $[Co(CLHOsar)]^{3+}$ | 3.7 | 0.21 | 0.039 | 0.69 | 3.0 | 0.19 |
| $[Co(diCLsar)]^{3+}$ | 4.6 | 0.24 | 0.043 | 0.83 | 3.8 | 0.18 |
| $[Co(diAMsar)]^{3+}$ | 1.1 | 0.07[1] | 0.012 | 0.18 | 0.9 | 0.17 |
| *lel*$_3$-$[Co(diAMchar)]^{3+}$ | 1.9 | 0.12 | 0.047 | 0.74 | 1.2 | 0.39 |
| $[Co(CLNOsar)]^{3+}$ | 5.8 | 0.29 | $0.05_2$ | 1.0 | 4.8 | 0.18 |
| $[Co(diNOsar)]^{3+}$ | 7.7 | 0.35 | 0.070 | 1.5 | 6.2 | 0.20 |
| $[Co(AZAcapten)]^{3+}$ | 15.1 | 0.51 | | | | |
| $[Co(AMcapten)]^{3+}$ | 12.5 | 0.46 | 0.06 | 1.7 | 11 | 0.13 |
| $mv^{2+}$ | 11.0 | 0.43 | 0.07[e] | 11.0 | | |

[a] Reaction conditions are described in Table I. [b] Calculation value at $2 \times 10^{-3}$ M Co(III), $k_1 = 2.9 \times 10^6\ s^{-1}$. [c] Quantum yield measurements indicated some decomposition of the sensitizer. However, for a given complex, the correspondence of quantum yields and hydrogen-production rates between the two sensitizers indicated that this did not cause a serious error. Quantum yields were generally obtained at $4 \times 10^{-3}$ M in cage complex and extrapolated to $2 \times 10^{-3}$ M, corrections being made for absorption by the Co(II) complexes and the filtering effect of the Co(III) complexes. [d] Calculated by assuming cage-escape yields were unity. [e] Launikonis, A.; Mau, A. W.-H.; Sasse, W. H. F., unpublished results. The low quantum yields of $mv^{+\cdot}$ were due to low cage-escape yields. [f] The quantum yields is low here presumably due to reduction of the $-NO_2$ substituents with Co(II). This is not as great a problem with the other nitro-substituted cage complexes with more positive Co(III)/Co(II) redox potentials.

of complex) were also performed on $[Co(sep)]^{3+}$ and $[Co(CLsar)]^{3+}$. Separations of complexes were performed on SP-Sephadex C-25 cation-exchange resin with use of eluant conditions previously described for separating the cage complexes.[4-14]

In an experiment designed to determine how quickly the Co(II) cage complexes react with the platinum catalyst, the Pt(PVA) catalyst (2.5 × $10^{-6}$ M Pt, final concentration) and $[Co(sep)]^{2+}$ ($10^{-5}$ M, final concentration) were mixed under an atmosphere of deoxygenated ($Cr^{2+}$) $N_2$ with a hand mixer.[61] The formation of Co(III) was monitored spectrophotometrically by following the growth in the ligand to metal charge-transfer (LMCT) transition of the Co(III) complex (240 nm).

## Results

Redox potentials of the cage complexes, their quenching rate constants ($k_q$), and quantum yields for quenching (by both electron and energy transfer) are collated in Tables I and II for $[Ru(bpy)_3]^{2+}$ and $[Ru(4,4'\text{-}Me_2bpy)_3]^{2+}$, respectively. Quenching rate constants of $[Ru^*(bpy)_3]^{2+}$ varied from $10^7$ to $10^9\ M^{-1}\ s^{-1}$ and generally increased as the redox potential of the Co(III)/Co(II) couple was made more positive. The methyl-substituted ruthenium complex exhibited larger quenching constants in its excited state (by a factor of ~2); however, its lifetime ($\tau$ = 350 ns) was shorter than that of $[Ru^*(bpy)_3]^{2+}$ (640 ns) under the experimental conditions (pH 5.0, AcOH/AcO$^-$ buffer, 20 °C). The maximum possible Co(II) quantum yields ($\Phi_{max}$) were calculated from these quenching constants according to the equation $\Phi_{max} = k_q[ETA]/(k_q[ETA] + k_1)$, where $k_1 = 1/\tau$. These were found to be comparable for the two sensitizers (Tables I and II). Generally, oxidative quenching decreased in comparison to energy-transfer quenching as the potential for the Co(III)/Co(II) couple was made more negative. For the $[Co(capten)]^{3+}$ cage complexes and the sar complexes with potentials more positive than −0.34 V vs. NHE, quenching of $[Ru^*(bpy)_3]^{2+}$ occurs almost exclusively via an oxidative pathway; therefore, back electron transfer within the solvent cage before the products escape (i.e. solvent-cage-escape yields below unity) does not limit oxidative-quenching quantum yields, at least with these complexes. Conversely, it appears that the oxosar complexes quench the excited states almost entirely by energy transfer. Increasing the concentration of edta beyond $10^{-2}$ M does not influence Co(II) quantum yields significantly for $[Co(sep)]^{3+}$, which indicates that the quantum yields are not limited by the back-reaction (3) for the concentrations of edta used. As shown earlier,[26] by examination of the recovery of the Ru(II) signal during flash photolyses of $[Ru(bpy)_3]^{2+}$, the rate of the back-reaction was estimated as $5 \times 10^8\ M^{-1}\ s^{-1}$ for $[Co(AZAcapten)]^{2+}$ and $2 \times 10^9\ M^{-1}\ s^{-1}$ for $[Co(sep)]^{2+}$. However, the accuracy of these values was limited by other competing side reactions causing deviations from second-order kinetics. Generally, quantum yields for Ru(III) obtained by flash photolysis were in agreement with those determined for Co(II) determined by continuous irradiation although the former measurements were not as accurate. No attempt was made to monitor any reactions between oxidized species derived from edta and Co(II) because the molecular extinction coefficient of Co(II) is far too small to allow reliable measurements.

**Table III.** Hydrogen-Production Experiments for $[Ru(bpy)_3]^{2+}$ as Sensitizer at pH 5.0[a]

| electron-transfer agent | rel rate[b] | yield, $\mu$mol/mL[c] |
|---|---|---|
| $[Co(HYMEoxosar\text{-}H)]^{2+}$ | not detected | nil |
| $[Co(CMMEabsar)]^{3+}$ | not detected | nil |
| $[Co(EFMEoxosar\text{-}H)]^{2+}$ | not detected | nil |
| $[Co(sar)]^{3+}$ | 3.2 | 0.9 |
| $[Co(AZAMEsar)]^{3+}$ | 13 | 3.0 |
| $[Co(AMMEsar)]^{3+}$ | 9 | 2.4 |
| *lel*$_3$-$[Co(diAZAchar)]^{3+}$ | 33 | 7.5 |
| $[Co(CLsar)]^{3+}$ | 36 | 8.2 |
| $[Co(sep)]^{3+}$ | 31 | 7.1 |
| $[Co(MENOsar)]^{3+}$ | 4.2[d] | 0.78[d] |
| $[Co(CLHOsar)]^{3+}$ | 31 | 6.8 |
| $[Co(diCLsar)]^{3+}$ | 22 | 5.0 |
| *lel*$_3$-$[Co(diAMchar)]^{3+}$ | 3.9 | 1.0 |
| $[Co(diAMsar)]^{3+}$ | 4.7 | 0.7 |
| $[Co(CLNOsar)]^{3+}$ | 14.2[d] | 2.5[d] |
| $[Co(diNOsar)]^{3+}$ | not detected | nil |
| $[Co(AZAcapten)]^{3+}$ | not detected | nil |
| $[Co(AMcapten)]^{3+}$ | not detected | nil |
| methylviologen(2+) | 100 | 19.6 |
| benzylviologen(2+) | 5 | 1.5[49] |

[a] Reaction conditions: 20 °C, $6 \times 10^{-5}$ M $[Ru(bpy)_3]^{2+}$, $2 \times 10^{-3}$ M ETA, $2 \times 10^{-2}$ M edta, $5 \times 10^{-5}$ M Pt(PVA), pH 5.0 (HOAc/OAc$^-$), Xe lamp 150 W, 5 mL total volume. [b] Relative rate of initial hydrogen production vs. 100% for methylviologen. [c] 2-h irradiation. [d] Complicated by reactions of nitro substituent with Pt(PVA) and poisoning of the catalyst.

Because of the complexity of the system, the rate of the forward reaction (4) was studied with $[Co(sep)]^{2+}$. The oxidation of $[Co(sep)]^{2+}$ in the presence of Pt(PVA) was rapid, considering the small thermodynamic driving force ($\Delta G \approx 0$ at pH 5.0). Under the reaction conditions, ([Pt(PVA)] = $2.5 \times 10^{-6}$ M Pt;[49-52] $[[Co(sep)]^{2+}] = 10^{-5}$ M) pseudo-first-order kinetics were observed

---

[61] Similar in design to that reported by: Inoue, Y.; Perrin, D. D. *J. Phys. Chem.* **1962**, *66*, 1689.

**Table IV.** Hydrogen-Production Experiments for $[Ru(4,4'\text{-}Me_2bpy)_3]^{2+}$ as Sensitizer at pH 5.0[a]

| electron-transfer agent | rel rate[b] | yield, μmol/mL[c] |
|---|---|---|
| $[Co(HYMEoxosar\text{-}H)]^{2+}$ | not detected | nil |
| $[Co(CMMEabsar)]^{3+}$ | 0.27 | 0.07 |
| $[Co(EFMEoxosar\text{-}H)]^{2+}$ | 0.12 | 0.03 |
| $[Co(sar)]^{3+}$ | 4.6 | 1.3 |
| $[Co(AZAMEsar)]^{3+}$ | 6.4 | 1.8 |
| $[Co(AMMEsar)]^{3+}$ | 6.0 | 1.5 |
| *lel*$_3$-$[Co(diAZAchar)]^{3+}$ | 15 | 4.3 |
| $[Co(CLsar)]^{3+}$ | 26 | 7.4 |
| $[Co(sep)]^{3+}$ | 9.8 | 2.4 |
| $[Co(MENOsar)]^{3+}$ | 0.45[d] | 0.01[d] |
| $[Co(CLHOsar)]^{3+}$ | 12 | 3.6 |
| $[Co(diCLsar)]^{3+}$ | 5.5 | 1.4 |
| *lel*$_3$-$[Co(diAMchar)]^{3+}$ | 6 | 1.4 |
| $[Co(diAMsar)]^{3+}$ | 1.3 | 0.2 |
| $[Co(CLNOsar)]^{3+}$ | not detected[d] | nil[d] |
| $[Co(diNOsar)]^{3+}$ | not detected | nil |
| $[Co(AZAcapten)]^{3+}$ | not detected | nil |
| $[Co(AMcapten)]^{3+}$ | not detected | nil |
| methylviologen(2+) | 13 | 4.5 |

[a] Reaction conditions as quoted in Table III except $[Ru(4,4'\text{-}Me_2bpy)_3]^{2+}$ was used as sensitizer. [b] Relative rate of initial hydrogen production vs. 100% for $[Ru(bpy)_3]^{2+}/mv^{2+}$. [c] 2-h irradiation. [d] Complicated by reactions of nitro substituent with Pt(PVA) and poisoning of the catalyst.

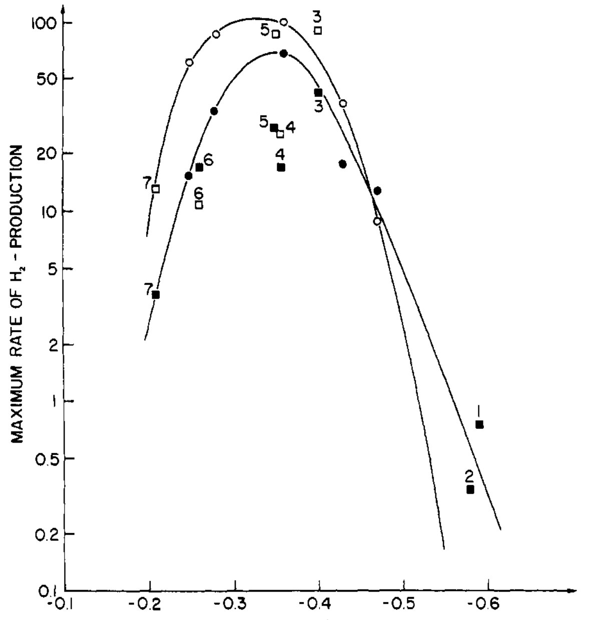

**Figure 1.** log (relative maximum hydrogen-production rate) vs. potential of Co(III)/Co(II) couples with both $[Ru(bpy)_3]^{2+}$ (open symbols) and $[Ru(4,4'\text{-}Me_2bpy)_3]^{2+}$ (closed symbols) as sensitizers at pH 5.0. Complexes denoted by ○ or ● are sar cage complexes while other complexes on the curve are as follows: (1) $[Co(CMMEabsar)]^{3+}$; (2) $[Co(EFMEoxosar\text{-}H)]^{2+}$; (3) $[Co(diAZAchar)]^{3+}$; (4) $[Co(AMMEsar)]^{3+}$; (5) $[Co(sep)]^{3+}$; (6) $[Co(diAMchar)]^{3+}$; (7) $[Co(diAMsar)]^{3+}$. Reaction conditions are described in Tables III and IV. All relative hydrogen-production rates are standardized to 100% for the $mv^{2+}/[Ru(bpy)_3]^{2+}$ system at 2 × $10^{-3}$ M in ETA.

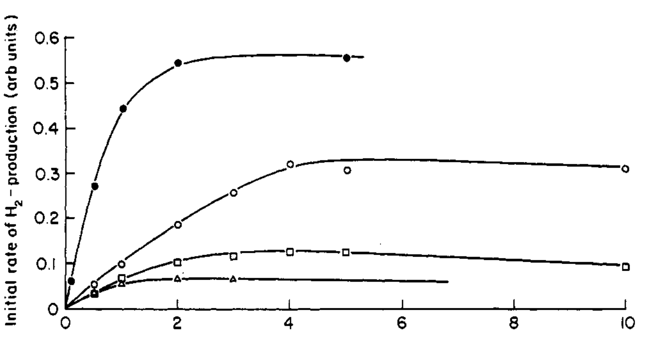

**Figure 2.** ETA concentration dependencies of the maximum hydrogen-production rates for the systems $[Ru(bpy)_3]^{2+}/mv^{2+}$ (●), $[Ru(bpy)_3]^{2+}/[Co(CLsar)]^{3+}$ (○), $[Ru(4,4'\text{-}Me_2bpy)_3]^{2+}/mv^{2+}$ (△), and $[Ru(4,4'\text{-}Me_2bpy)_3]^{2+}/[Co(CLsar)]^{3+}$ (□).

**Table V.** Effect of Concentration of Platinum Catalyst and of Co(III) on Hydrogen-Production Rate for the $[Ru(bpy)_3]^{2+}/[Co(CLsar)]^{3+}/Pt(PVA)/edta$ System[a]

| $[[Co(CLsar)]^{3+}]$, M | [Pt(PVA)], M | rel rate[b] | yield of $H_2$,[c] mL |
|---|---|---|---|
| 5 × $10^{-4}$ | 5 × $10^{-5}$ | 10 | 0.22 |
| 1 × $10^{-3}$ | 5 × $10^{-5}$ | 20 | 0.40 |
| 2 × $10^{-3}$ | 2.5 × $10^{-6}$ | 25 | 0.303 |
| 2 × $10^{-3}$ | 5 × $10^{-6}$ | 37 | 0.447 |
| 2 × $10^{-3}$ | 1 × $10^{-5}$ | 36 | 0.57 |
| 2 × $10^{-3}$ | 2.5 × $10^{-5}$ | 36 | 0.70 |
| 2 × $10^{-3}$ | 5 × $10^{-5}$ | 36 | 0.77 |
| 2 × $10^{-3}$ | 1 × $10^{-4}$ | 37 | 0.82 |
| 3 × $10^{-3}$ | 5 × $10^{-5}$ | 51 | 1.09 |
| 4 × $10^{-3}$ | 5 × $10^{-5}$ | 65 | 1.35 |
| 4 × $10^{-3}$ | 1 × $10^{-4}$ | 69 | 1.27 |
| 5 × $10^{-3}$ | 5 × $10^{-5}$ | 63 | 1.36 |
| $10^{-2}$ | 5 × $10^{-5}$ | 70 | 1.41 |
| $10^{-2}$ | 1 × $10^{-4}$ | 65 | 1.34 |

[a] Reaction conditions were the same as those reported in Tables III and IV. [b] Relative rate of initial hydrogen production vs. 100 for 2 × $10^{-3}$ M $mv^{2+}$ under identical conditions. [c] Yield of $H_2$ after 75 min of irradiation for 5 mL of solution.

for Co(III) production with a half-life of 0.35 s. Concomitant hydrogen production was observed with Co(II) solutions under these conditions. Tables III and IV contain the relative maximum rates of production and yields of $H_2$ for the two different photosensitizers at pH 5.0. The dependence of maximum hydrogen production on the redox potential of the Co(III)/Co(II) couples is depicted in Figure 1 ([ETA] = 2 × $10^{-3}$ M) for both dyes. The most efficient ETA for both systems was $[Co(CLsar)]^{3+}$, although the curve for $[Ru(4,4'\text{-}Me_2bpy)_3]^{2+}$ was shifted to more negative potentials. Plots of the relative maximum rates of hydrogen production vs. the concentration of ETA ($mv^{2+}$, $[Co(CLsar)]^{3+}$) for the two ruthenium complexes are depicted in Figure 2 at a constant concentration of catalyst ([Pt(PVA)] ≈ 5 × $10^{-5}$ M Pt). For both sensitizers, the hydrogen production rates attain maximum values at 4 × $10^{-3}$ M for the cage complexes and at 2 × $10^{-3}$ M for methyl viologen.

For platinum concentrations between 5 × $10^{-6}$ and 1 × $10^{-4}$ M, the maximum rate of hydrogen production was effectively unaltered for $[Co(CLsar)]^{3+}$ (2 × $10^{-3}$ M), but during the later stages of irradiation, the rate of hydrogen production decreased more rapidly as the Pt(PVA) concentration was decreased (i.e. the sacrificial cycles become shorter lived). When the Pt(PVA) concentration was reduced below 2.5 × $10^{-6}$ M Pt, both the maximum rate of hydrogen production and the volume of hydrogen produced in a given period of time decreased rapidly. These experiments are summarized in Table V and Figure 3.

Under optimal conditions for $H_2$ production at pH 5.0, the cage complexes $[Co(CLsar)]^{3+}$ and $[Co(sep)]^{3+}$ are about as efficient as methylviologen. These results agree with the quantum yields of formation of the reduced species and the measured quenching constants. Analogous experiments with rhodium cage complexes[54] did not yield any hydrogen, which was consistent with a lack of observable quenching of $[Ru^*(bpy)_3]^{2+}$.

During long-term irradiations at pH 5.0, the rate of $H_2$ production fell off more rapidly (per mole of $H_2$ produced) with the cage complexes ($[Co(CLsar)]^{3+}$, $[Co(sep)]^{3+}$) than with methylviologen (Figure 4). The rate at which this decay occurred did not appear to depend on the concentration of $[Co(CLsar)]^{3+}$ (2 × $10^{-3}$ and 4 × $10^{-3}$ M), and there was no noticeable degradation of the cage complexes (HPLC and LC) even after 10-h irradiation. The extrapolated turnover numbers (>5000) derived from these experiments were at least 2 orders of magnitude greater

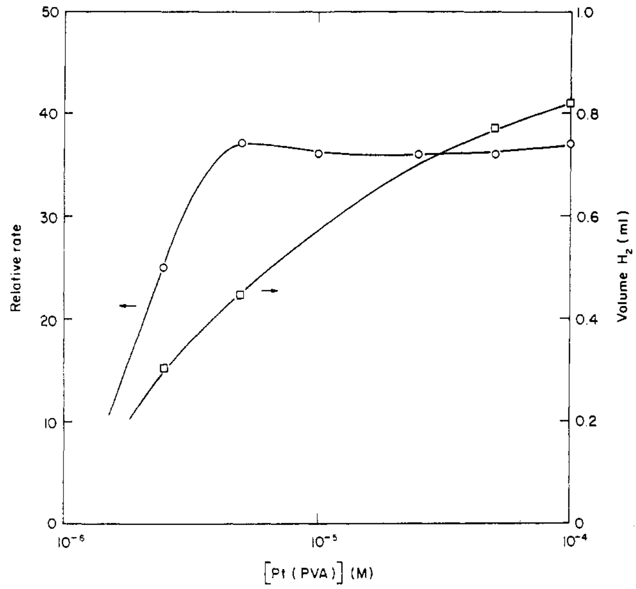

**Figure 3.** Effect of Pt(PVA) concentration on the hydrogen-production rates (○) and yields of hydrogen (□) with $[Co(CLsar)]^{3+}$ ($2 \times 10^{-3}$ M) and $[Ru(bpy)_3]^{2+}$. Conditions are contained in Table V.

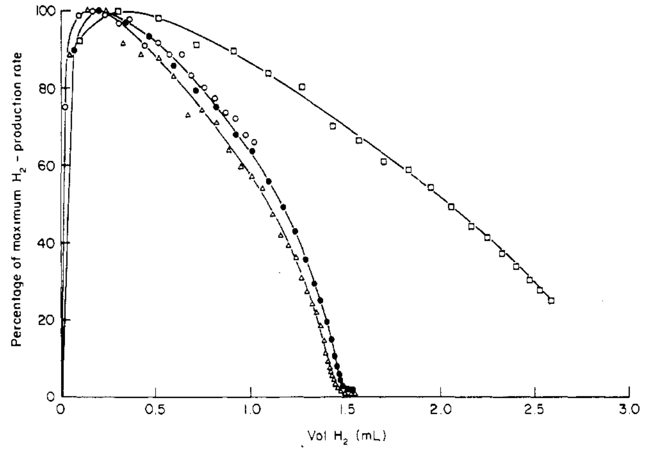

**Figure 4.** Variation of hydrogen-production rates vs. volume of hydrogen produced for $[Ru(bpy)_3]^{2+}$ with the ETA's $[Co(CLsar)]^{3+}$ ($2 \times 10^{-3}$ M, ●; $4 \times 10^{-3}$ M, ○), $[Co(sep)]^{3+}$ ($2 \times 10^{-3}$ M, △), and $mv^{2+}$ ($2 \times 10^{-3}$ M, □). All hydrogen-production rates are standardized to the maximum rate for each system being 100%.

than those observed with $mv^{2+}$.[26] This value constitutes a lower limit; limiting values have not yet been sought due to loss in catalyst activity over prolonged irradiation.

The pH value at which the maximum rate of hydrogen production was observed was lower for complexes with a more positive reduction potential (Table VI). For example, with $[Co(AMMEsar)]^{3+}$ and $[Co(sep)]^{3+}$, this rate reached its maximum value at pH 5.0 when edta was used as a sacrificial electron donor, but with $[Co(sar)]^{3+}$, the maximum value occurred at pH 6.6. The maximum rate of hydrogen production with $[Co(AMMEsar)]^{3+}$ was less sensitive to changes in pH than it was with the other complexes.[26] When $[Co(AZAcapten)]^{3+}$ was used as an electron-transfer agent and the photolysis compartment was connected to a second solution at pH 0 via a platinum electrode, hydrogen formed readily.[26]

Photolysis experiments involving $[Ru(4,4'\text{-}Me_2bpy)_3]^{2+}$ indicated that the $[Ru^*(4,4'\text{-}Me_2bpy)_3]^{2+}$ and/or the $[Ru(4,4'\text{-}Me_2bpy)_3]^{3+}$ ions were less stable than analogous complexes containing the bpy ligand. This was shown by a decrease in the concentration of $[Ru(4,4'\text{-}Me_2bpy)_3]^{2+}$ during the continuous irradiation used for quantum yield measurements and by a more rapid decay of $H_2$ production than observed with analogous systems containing $[Ru(bpy)_3]^{2+}$. Therefore, Co(II) quantum yield measurements with $[Ru(4,4'\text{-}Me_2bpy)_3]^{2+}$ are somewhat more

**Table VI.** pH Dependence of $H_2$ Production with $[Ru(bpy)_3]^{2+}$ as Sensitizer[a]

| cage complex | pH | rel rate[b] | vol of $H_2$, mL |
|---|---|---|---|
| $[Co(sep)]^{3+}$ | 2.6 | 0.33 | 0.0026 |
| | 3.7 | 6.2 | 0.10 |
| | 5.0 | 31 | 0.80 |
| | 6.65 | 11 | 0.18 |
| | 7.6 | 2.3 | 0.04 |
| $[Co(sar)]^{3+}$ | 3.7 | 0.65 | 0.0059 |
| | 5.0 | 3.2 | 0.03 |
| | 6.65 | 6.1 | 0.06 |
| | 7.8 | 0.34 | 0.002 |
| $[Co(AMMEsar)]^{3+}$ | 3.7 | 4.4 | 0.07 |
| | 5.0 | 9 | 0.15 |
| | 6.65 | 6.0 | 0.09 |
| | 7.80 | 1.0 | 0.01 |

[a] Irradiation conditions: $[[Ru(bpy)_3]^{2+}] = 6 \times 10^{-5}$ M; [edta] = $2 \times 10^{-2}$ M; $[Pt(PVA)] = 5 \times 10^{-5}$ M; $[Co(III)] = 2 \times 10^{-3}$ M. [b] Relative rate vs. 100 for $[Ru(bpy)_3]^{2+}/mv^{2+}$ system at the same concentrations. [c] Volume of hydrogen produced from a 5-mL sample.

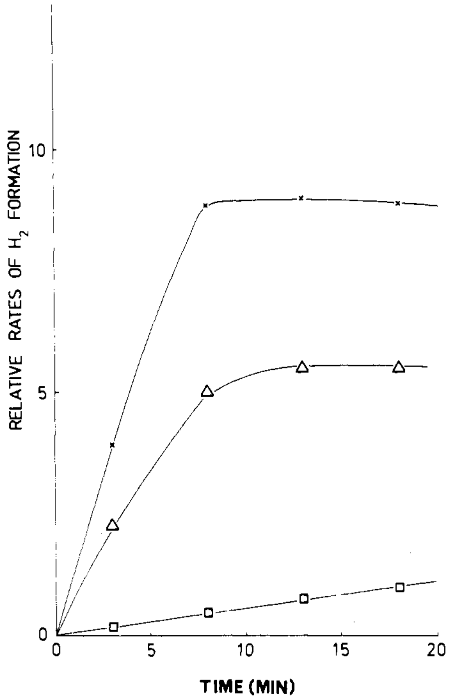

**Figure 5.** Variation in hydrogen-production rates with time with $[Ru(bpy)_3]^{2+}$ as sensitizer for the following ETA's at $2 \times 10^{-3}$ M concentration: $[Co(diAMsar)]^{3+}$ (□); $[Co(diCLsar)]^{3+}$ (△); $[Co(CLsar)]^{3+}$ (×).

difficult and less reliable than with $[Ru(bpy)_3]^{2+}$. However, in most cases decomposition was not important at the early stages. Hence, the quantum yields of formation of Co(II), measured in the absence of Pt, are consistent with the rates of formation of $H_2$ in this region. Solutions of complexes with redox potentials more positive than that of $[Co(sep)]^{3+/2+}$ were bleached because of a buildup of Co(II) during $H_2$-production experiments. This buildup in Co(II) is consistent with a Nernstian dependence, and with these complexes the rate of hydrogen production took a longer time to reach its maximum value (Figure 5), as expected from the hydrogen-production equilibrium (4). The concentration dependencies of the quantum yields of several cage complexes yielded constant values of $k_2$, also as expected (Table VII). In addition, Table VII shows that higher concentrations of edta have no marked effect on the $k_2$ values obtained for the $[Co(sep)]^{3+}$ system.

Finally, at the concentration $[Co(CLsar)]^{3+}$ where the $H_2$-production rate reaches its maximum value, the overall quantum yields of quenching (obtained from Stern–Volmer analyses) of the excited states were 26% and 25% for $[Ru^*(bpy)_3]^{2+}$ and $[Ru^*(4,4'\text{-}Me_2bpy)_3]^{2+}$, respectively.

**Table VII.** Concentration Dependencies of Quantum Yields for $[Ru(bpy)_3]^{2+}$ as Sensitizer[a]

| complex | concn, M | Φ(Co(II)) | $k_2$(calcd), $M^{-1}\ s^{-1}$ |
|---|---|---|---|
| $[Co(CLsar)]^{3+}$ | $1 \times 10^{-3}$ [b] | 0.031 | $5.1 \times 10^7$ |
| | $2 \times 10^{-3}$ [b] | 0.052 | $4.4 \times 10^7$ |
| | $4 \times 10^{-3}$ [b] | 0.091 | $4.0 \times 10^7$ |
| | $8 \times 10^{-3}$ [b] | $0.17_4$ | $4.2 \times 10^7$ |
| $[Co(sep)]^{3+}$ | $2 \times 10^{-3}$ [c] | 0.040 | $3.3 \times 10^7$ |
| | $8 \times 10^{-3}$ [c,d] | 0.164 | $3.9 \times 10^7$ |
| $[Co(CLHOsar)]^{3+}$ | $2 \times 10^{-3}$ [b] | $0.19_2$ | $1.9 \times 10^8$ |
| | $2 \times 10^{-3}$ [c] | $0.19_0$ | $1.9 \times 10^8$ |
| | $4 \times 10^{-3}$ [c] | $0.28_5$ | $1.6 \times 10^8$ |

[a] All measurements performed at an excitation wavelength of 405 nm, unless otherwise stated. [b] Under normal photolysis conditions $2 \times 10^{-2}$ M edta. [c] 460-nm excitation. [d] 0.1 M edta.

## Discussion

**Quenching of Triplet Excited States of $[Ru(bpy)_3]^{2+}$ and $[Ru(4,4'\text{-}Me_2bpy)_3]^{2+}$ by Cobalt Cage Complexes.** The lowest lying triplet excited states of $[Ru(bpy)_3]^{2+}$ and $[Ru(4,4'\text{-}Me_2bpy)_3]^{2+}$ are reported to have lifetimes of 600 and 330 ns, respectively, at 25 °C.[62] Similar excited-state lifetimes were observed here at 20 °C in NaOAc/AcOH buffers (pH 5.0) (640 and 350 ns). These excited states may be quenched by oxidative, reductive, and/or energy-transfer routes depending on the quenching agent added.[53,63] Since there is no evidence that the Co(III) cage complexes can be oxidized to Co(IV),[14,15] quenching was restricted to oxidative and energy-transfer pathways (reactions 2 and 2′, respectively).

Oxidative quenching is thermodynamically favored with both sensitizers ($[Ru^*(bpy)_3]^{2+}$, −0.84 V; $[Ru(4,4'\text{-}Me_2bpy_3)]^{2+}$, −1.00 V)[62] and should become more favored as the Co(III)/Co(II) redox potential is made more positive. This trend is clearly shown by the quenching constants ($k_q$) and quantum yields (Φ(Co(II))) for the substituted cobalt sar complexes (Tables I and II). For $[Ru(bpy)_3]^{2+}$, the values of the quenching constants tend to increase as the Co(III)/Co(II) potential becomes more positive because the oxidative pathway (Ru(III) formation) becomes more favored. With the sar cage complexes, inefficient solvent-cage escape has been ruled out as a major cause for low Co(II) quantum yields with $[Ru(bpy)_3]^{2+}$ as sensitizer, since the sar complexes with redox potentials more positive than −0.35 V vs. NHE were found to quench almost exclusively (≳95%) by electron transfer. Similar observations were made with $[Co(AZAcapten)]^{3+}$. The partially protonated amine-substituted cage complexes $[Co(diAMsar)]^{3+}$, $[Co(diAMchar)]^{3+}$, and $[Co(AMcapten)]^{3+}$ were exceptions to this rule, for reasons which we do not understand at present. The remainder of the quenching was ascribed to energy transfer,[26] a conclusion that has been supported by more recent work.[64] By contrast, with the $[Ru^*(4,4'\text{-}Me_2bpy)_3]^{2+}$ ion, the increased quenching rate by cage complexes could be accounted for by an increase in the energy-transfer efficiency. Solvent-cage-escape yields below unity may also contribute to the relatively low proportion of apparent electron-transfer quenching. Solvent-cage-escape yields for $mv^{+\cdot}$ are 50% lower with the substituted sensitizer than with $[Ru(bpy)_3]^{3+}$, and this may also hold for quenching by the cage complexes, especially since the highest observed Co(II) quantum yield was below 0.5 with $[Ru(4,4'\text{-}Me_2bpy)_3]^{2+}$, whereas with $[Ru(bpy)_3]^{2+}$ it reached unity in some instances. We note also that the quenching rate constants for $[Ru^*(4,4'\text{-}Me_2bpy)_3]^{2+}$ are larger than those observed with $[Ru^*(bpy)_3]^{2+}$. This arises because $[Ru^*(4,4'\text{-}Me_2bpy)_3]^{2+}$ is a more powerful reductant than is $[Ru^*(bpy)_3]^{2+}$ (by 0.16 V);[62] therefore, the thermodynamic driving forces for electron transfer are greater, leading to higher quenching constants.

**Table VIII.** Self-Exchange Rates of Cobalt Cage Complexes at 25 °C

| complex | medium | $k_{ex}$, $M^{-1}\ s^{-1}$ | ref |
|---|---|---|---|
| $[Co(CMMEabsar)]^{3+/2+}$ | 0.2 M NaCl | 7.3 ± 0.3 | 25 |
| $[Co(EFMEoxosar\text{-}H)]^{2+/+}$ | 0.2 M NaCl | 5.3 | 11 |
| $[Co(sar)]^{3+/2+}$ | 0.2 M NaCl | 2.1 ± 0.2 | 20 |
| $[Co(AZAMEsar)]^{3+/2+}$ | 0.2 M NaCl | 2.9 | 4 |
| *lel*$_3$-$[Co(diAZAchar)]^{3+/2+}$ | 0.2 M NaCl | 22 ± 2 | 25 |
| $[Co(CLMEsar)]^{3+/2+}$ | 0.2 M NaCl | 2.4 ± 0.3 | 25 |
| $[Co(diCLsar)]^{3+/2+}$ | 0.2 M NaCl | 3.0 ± 0.3 | 25 |
| $[Co(sep)]^{3+/2+}$ | 0.2 M NaCl | 5.1 ± 0.3 | 4 |
| | 0.5 M NaCl | 11.5 | |
| $[Co(diAMsar)]^{3+/2+}$ | 0.2 M $LiClO_4$ (pH 7.5) | 0.50 ± 0.01 | 20 |
| $[Co(diAMsarH_2)]^{5+/4+}$ | 0.2 M $LiClO_4$ (pH 1.0) | 0.024 ± 0.002 | 20 |
| *lel*$_3$-$[Co(diAMchar)]^{3+/2+}$ | 0.2 M $NaCF_3SO_3$ (pH 7.5) | 1.1 ± 0.2 | 8 |
| *lel*$_3$-$[Co(diAMcharH_2)]^{5+/4+}$ | 0.2 M $Na(H)ClO_4$ | 0.038 ± 0.003 | 8 |
| $[Co(AZAcapten)]^{3+/2+}$ | ~0.2 M NaCl | 4500 ± 300 | 22 |

It is believed that energy transfer in coordination complexes involves a concerted two-electron-transfer process with retention of parity.[65] Thus it would depend on both the energy separations between the two systems and the relative energies of the ground and excited states of both ions. The lower Co(II) quantum yields found with $[Ru^*(4,4'\text{-}Me_2bpy)_3]^{2+}$ could then also be explained if energy transfer to the cage complexes is more favored from $[Ru^*(4,4'\text{-}Me_2bpy)_3]^{2+}$ than from $[Ru^*(bpy)_3]^{2+}$. The shorter excited-state lifetime of the methyl-substituted ion further reduces the yield of Co(II) with this sensitizer. Both these factors tend to lower the quantum yields for Co(II) despite the more favorable thermodynamics for its formation. However, at present we cannot distinguish between energy transfer and back electron transfer within the solvent cage, i.e., before escape from the solvent cage, for reactions involving $[Ru^*(bpy)_3]^{2+}$ and the Co(III) cages.

The sensitivity of the competition between energy-transfer and electron-transfer quenching is well illustrated for the $[Co(sep)]^{3+}$ and $[Co(CLsar)]^{3+}$ complexes. Both have similar electron self-exchange rate constants (Table VIII) and redox potentials (Table I), and their spectra are also similar (Table IX). However, $[Co(sep)]^{3+}$ is more efficient in quenching $[Ru^*(bpy)_3]^{2+}$ by energy transfer than is $[Co(CLsar)]^{3+}$. This effect is even greater for $[Ru^*(4,4'\text{-}Me_2bpy)_3]^{2+}$, suggesting, possibly, that the precise locations of triplet levels on the absolute energy scale is important. Table IX shows that the calculated lowest triplet energies of the Co(III) cage complexes only differ slightly, which would again support the notion that fine tuning of energy levels is important. This aspect will be addressed in more detail in a subsequent publication.

The effects of the self-exchange rates (Table VII) of the Co(III)/Co(II) couples were also examined in relation to the amount of oxidative quenching compared to energy-transfer quenching. Particularly illuminating in this respect were the quenching constants observed for the cage complexes with the $N_3S_3$ (capten) ligands. Quenching constants observed with these complexes were a factor of 2 larger than those expected with sar complexes of the same redox potentials. However, the rate constants for electron self-exchange are approximately 3 orders of magnitude larger than those observed for the sar cage complexes.[4,20,22] Clearly, the rate of electron-transfer quenching depends on the self-exchange rates, as expected.[64] Further, *lel*$_3$-$[Co(diAZAchar)]^{3+}$ and $[Co(sep)]^{3+}$ have similar quenching constants despite the weaker oxidizing ability of the former complex. Again, such differences can be attributed to differences in the self-exchange rates (Table VIII).[4,25] However, with these complexes energy-transfer quenching makes a significant contribution, which seems to be very sensitive to small perturbations in electronic structures of the cobalt complexes and the sensitizer. The short lifetime of the triplet ligand field states of the Co(III) complexes (≲1 ns) makes their utilization for

---

(62) Sutin, N.; Creutz, C. *Adv. Chem. Ser.* **1978**, *No. 168*, 1.
(63) Juris, A.; Gandolfi, M. T.; Manfrin, M. F.; Balzani, V. *J. Am. Chem. Soc.* **1976**, *98*, 1047.
(64) Mok, C.-Y.; Zanella, A. W.; Creutz, C.; Sutin, N. *Inorg. Chem.* **1984**, *23*, 2891.
(65) Scandola, F.; Balzani, V. *J. Chem. Educ.* **1983**, *60*, 814.

**Table IX.** Ligand Field Spectra of Co(III) Cage Complexes

| complex | $^1A_1 \rightarrow {}^3T_1{}^{a,b}$ | $^1A_1 \rightarrow {}^3T_2{}^{a,b}$ | $^1A_1 \rightarrow {}^1T_1{}^{a}$ | $^1A_1 \rightarrow {}^1T_2{}^{a}$ | $\Delta^c$ | $B^c$ |
|---|---|---|---|---|---|---|
| $[Co(XYsar)]^{n+}$ | 15 540 (644) | 19 140 (522) | 21 100 (474) | 29 100 (344) | 22 100 | 580 |
| $[Co(AZAMEsar)]^{3+}$ | 15 620 (640) | 19 730 (507) | 21 320 (469) | 29 240 (342) | 22 350 | 572 |
| $[Co(sep)]^{3+}$ | 15 380 (650) | 19 490 (513) | 21 200 (472) | 29 400 (340) | 22 210 | 596 |
| $[Co(Xcapten)]^{n+}$ | 15 610 (641) | 18 680 (535) | 20 450 (489) | 27 140 (368.5) | 21 450 | 473 |
| $[Co(AZAcapten)]^{3+}$ | 15 830 (632) | 18 870 (530) | 20 450 (489) | 26 810 (373) | 21 440 | 446 |
| $[Co(XYabsar)]^{3+}$ | 16 360 (611) | 20 130 (497) | 21 800 (459) | 29 850 (335) | 22 850 | 580 |
| $[Co(XYoxosar\text{-}H)]^{2+}$ | | | 20 240 (494) | 28 990 (345) | 21 130 | 652 |
| $[Co(diAMchar)]^{3+}$ | | | 20 920 (478) | 29 410 (340) sh | 21 890 | ~624 |
| $[Co(diAMcharH_2)]^{5+}$ | | | 20 660 (484) | 28 570 (350) | 21 650 | 574 |
| $[Co(diAZAchar)]^{3+}$ | | | 20 830 (480) | 29 150 (343) | 21 800 | 610 |

[a] Frequency in $cm^{-1}$, with wavelength in nm in parentheses. [b] Calculated from Tanabe–Sugano diagram and values of $\Delta$ and $B$. [c] Calculated from $^1A_1 \rightarrow {}^1T_1$ ($\Delta - 4B + 86B^2/\Delta$) and $^1A_1 \rightarrow {}^1T_2$ ($\Delta + 12B + 2B^2/\Delta$) transitions, making allowances for second-order effects and assuming $C \approx 4B$. These values only give an order of the triplet levels as the $D_3$ symmetry of the complexes causes repulsion between the E components of the T excited states. Units are $cm^{-1}$.

hydrogen production extremely unlikely, and therefore, ways to minimize energy transfer are now being sought.

The above analysis implied that the absar cage complexes might quench the triplet excited states of the $[Ru(bpy)_3]^{2+}$ ions more efficiently by electron transfer than the corresponding sar complexes, since their lowest lying triplet excited states were calculated to be higher in energy and the electron self-exchange rate constants larger.[25] While both the above factors favor electron-transfer quenching, the redox potential of the absar complex studied was too negative for electron-transfer quenching to occur in effective competition with energy transfer. It is noteworthy that the $[Co(absar)]^{3+}$ complexes have the greatest energy differences between the lowest lying triplet state and the ground state of all the cage complexes used in this study (Table IX). However, this energy difference is still less than the corresponding energy difference between $[Ru(bpy)_3]^{2+}$ and $[Ru^*(bpy)_3]^{2+}$ (16 950 $cm^{-1}$) and therefore energy transfer cannot be excluded for any of the cage complexes. Hydrogen production was not detected with $[Co(CMMEabsar)]^{3+}$ as ETA and $[Ru(bpy)_3]^{2+}$ as sensitizer (Table III), but hydrogen was detected with $[Ru(4,4'\text{-}Me_2bpy)_3]^{2+}$. This is ascribed to the increased electron-transfer quenching for the latter, because of the higher reducing power of its excited state and/or because the energy difference between $[Ru^*(4,4'\text{-}Me_2bpy)_3]^{2+}$ and $[Ru(4,4'\text{-}Me_2bpy)_3]^{2+}$ is smaller than the corresponding energy difference between $[Ru^*(bpy)_3]^{2+}$ and $[Ru(bpy)_3]^{2+}$.

The effect of varying the charge on the cage complexes on the quenching rates was also examined. $[Co(diAMsar)]^{3+}$, $[Co(diAMchar)]^{3+}$, $[Co(AMMEsar)]^{3+}$, and $[Co(AMcapten)]^{3+}$ are partially protonated at pH 5, and it was observed that this partial protonation considerably decreased the quenching rate constants. This is explicable on the basis of increased coulombic work terms with increased charge of the ions, which is also reflected in experimental observations relating charge with self-exchange rate constants (Table VIII). Detailed experiments on the pH dependencies of such quenching experiments are currently in progress.[66]

We also note that the quenching constants observed in 0.5 M $NaClO_4$ were uniformly larger than those observed in the NaOAc/AcOH ($\mu$ = 0.15 M) buffer solutions. There appear to be at least two reasons for this. First, the ionic strength is greater in the $NaClO_4$ medium, thus reducing the electrostatic work terms involved in the bimolecular reaction. Second, the redox potentials of the cage complexes are more negative in the edta/acetate buffer solutions than with perchlorate as counterion. The shift of the redox potentials of cobalt complexes to more negative values occurs with all anions that have a greater tendency to hydrogen bond than the perchlorate ion.[67] Such behavior is attributed to ion association and/or changes in solvent structure.[67]

The char cage complexes (with their bulky cyclohexane groups) have larger quenching rate constants than the sar cage complexes. In fact, the rates are larger for a given potential, in agreement with the self-exchange measurements[8,25] (Table VIII). This would seem to imply that the quenching reactions are adiabatic. If the reactions were nonadiabatic, one would expect the quenching rate constants to be smaller for char cage complexes in comparison to those for sar cage complexes, due to changes in the distance of closest approach. However, it may transpire that the distances of closest approach for both sar and char complexes are similar, provided the ligand strands are specifically interlocked.[8,25] Such specificity would negate the previous arguments. It is also interesting that the back-reactions between Ru(III) and Co(II) are slower than those observed between Ru(III) and $mv^{+\cdot}$. This factor and the greater electrostatic repulsion in a solvent cage involving the former ions are likely to increase the efficiency of solvent-cage escape of the electron-transfer products with the cage complexes as ETA's. However, other factors may also be important, although not well understood. For instance, the factors responsible for the differences in solvent-cage-escape yields with methylviologen for the two sensitizers are, at present, not clear (Tables I and II). The fact that the back-reaction does not affect the quantum yield of electron transfer with the $[Co(sep)]^{3+}$ complex under the experimental conditions of hydrogen production is shown by a lack of edta dependence on Co(II) quantum yields above $10^{-2}$ M in edta (Table VII).

**Hydrogen-Production Experiments.** Sacrificial systems for photoreduction of water involving $[Ru(bpy)_3]^{2+}$ as sensitizer and viologens as electron-transfer agents have been studied in detail by many groups.[30-53] The reactions occurring in the system where edta is used as a sacrificial donor are described in Scheme I.

The cage complexes can be effective electron-transfer agents but are only useful for hydrogen production in a narrow potential range (Figure 1). The potential vs. initial rate of hydrogen production profile at pH 5.0 is much sharper than that observed for the viologen ions.[51,52] It drops off sharply at potentials more positive than ~−0.3 V because Co(II) ions with these potentials do not have the thermodynamic driving force to reduce $H_2O$ completely at pH 5.0. This behavior accounts for the finding (Figure 5) that cage complexes with redox potentials more positive than −0.35 V take longer to reach their maximum rates of hydrogen production than those with more negative potentials. The bleaching observed with such complexes is consistent with a buildup of Co(II) in solution, indicating that hydrogen production rates are thermodynamically controlled. There is no strong correspondence between rates of quenching and maximum rates of hydrogen production for these complexes. Instead, the rates of hydrogen production are controlled by the values of the Co(III)/Co(II) redox potential, again indicating thermodynamic control. This behavior is shown by the dropoff in maximum hydrogen production at positive redox potentials, which is illustrated in Figure 1.

The rapid reaction of Co(II) cage complexes with Pt(PVA) to regenerate Co(III) and $H_2$, even for those cage complexes with a small thermodynamic driving force for water reduction (i.e. $[Co(sep)]^{2+}$), shows that cage complexes with potentials more negative than −0.34 V vs. NHE produce $H_2$ at rates that are

---

(66) Hendry, A. J., work in progress.

(67) Lay, P. A.; Sargeson, A. M.; Hupp, J. T.; Weaver, M. J., manuscript in preparation.

controlled by the rate of production of Co(II). Since the hydrogen production is quantitative with respect to Co(II) quantum yields, and assuming second-order kinetics, the bimolecular rate constant is calculated to be of the order of $10^5$–$10^6$ $M^{-1}$ $s^{-1}$. This rate constant is only a lower limit since the platinum particles contain $\sim 10^3$ atoms,[68] and the actual rates may approach the diffusion-controlled limit of the solution. These experiments show that the Pt(PVA) catalyst has a very low overpotential for $H_2$ production with the cage complexes. By contrast, the overpotential for hydrogen production is much higher for benzylviologen with a redox potential similar to that of $[Co(CLsar)]^{3+}$ (Tables I and III). When the pH was lowered, hydrogen yields were increased for ions with redox potentials more positive than −0.35 V. however, edta becomes a weaker electron donor as the pH is lowered beyond $\sim 4$, because of protonation. This leads to competition between the back-reaction (3) and the scavenging reaction (5), causing a decrease in hydrogen yields. The dramatic drop in rate of hydrogen production observed with cage complexes with potentials more negative than −0.4 V (vs. NHE) is caused by the smaller thermodynamic driving force for electron transfer and increased competition with energy transfer in the quenching process; with $[Ru(4,4'\text{-}Me_2bpy)_3]^{2+}$ lower cage-escape yields may also contribute. With the viologens, where energy transfer does not occur, the rate of hydrogen production falls off more slowly with more negative redox potentials.[51,52] The $[Co(CLsar)]^{3+}$ and $[Co(sep)]^{3+}$ ions have similar electron-transfer rates, quenching constants, and electronic spectra, but the $[Co(CLsar)]^{3+}$ ion is better than the $[Co(sep)]^{3+}$ ion at electron-transfer quenching. This is reflected in the initial rates of hydrogen production and shows the former ion to be superior in these cycles, especially with $[Ru(4,4'\text{-}Me_2bpy)_3]^{2+}$ as a sensitizer. For the $[Co(AMMEsar)]^{3+}$ complex, the maximum hydrogen-production rate is much lower than those of complexes with similar Co(III)/Co(II) redox potentials (Figure 1). This arises from the low quenching rate constant, which we attribute to the higher charge of this species at pH 5.0. The production of hydrogen with this complex is less sensitive to pH changes[26] (Table VI) than with the other cage complexes. This is to be expected because the protonation/deprotonation equilibrium involving the apical amine group ($pK_a \approx 4$)[5,15] alters the redox potential of the cage complex in this pH region. Hence, the quenching rate (eq 2) and hydrogen-production equilibrium (eq 4) are also altered. A detailed examination of these factors will be given elsewhere.[66]

In general, the observed Co(II) quantum yields correlate well with the maximum rate of hydrogen production ($\Phi(^1/_2H_2) \approx \Phi(Co(II))$), showing that the electron-transfer quenching rates are reflected in the rates of hydrogen production. Unfortunately, the greatest rate of energy transfer for $[Ru^*(bpy)_3]^{2+}$ quenching occurs for those complexes that have the most suitable potentials for hydrogen generation (i.e. $[Co(CLsar)]^{3+}$ and $[Co(sep)]^{3+}$). This is so even though the percentage of energy-transfer quenching is lower for these complexes compared to those with more negative redox potentials. The above complexes would be required in concentrations of 0.01 and 0.1 M, for 50% and 90% quenching, respectively, with yields of Co(II) of 0.18 and 0.32, respectively. Contrary to the expectation that the amount of hydrogen produced in the cycles would follow the trends calculated for Co(II) formation, the maximum rate of hydrogen production reached a constant value at $4 \times 10^{-3}$ M in ETA for both sensitizers (where the quenching was only 25%). In general, the correspondence between $H_2$-production rates and $\Phi(Co(II))$ drops off as the Co(III) concentration increases. The activity of the Pt catalyst was not the limiting factor, since increasing the concentration of catalyst had little effect on the hydrogen-production rate (Table V, Figure 3). It was apparent that the internal filtering of light by excess Co(III) complex reduced the rate of hydrogen formation by reducing the frequency of excitation of the sensitizer. Since $\Phi(Co(II))$ is corrected for absorption by Co(III), this effect is only evident in the hydrogen-production rates. Thus, at higher concentration, the increased quenching by the cage complex was offset by the decreased intensity of light reaching the sensitizer.

It was hoped that $[Ru(4,4'\text{-}Me_2bpy)_3]^{2+}$ would be a better sensitizer for the hydrogen-production experiments since its visible absorption is at lower energy than that of $[Ru(bpy)_3]^{2+}$ and the $[Ru^*(4,4'\text{-}Me_2bpy)_3]^{2+}$ ion is a stronger reductant than is $[Ru^*(bpy)_3]^{2+}$.[62] A disadvantage of the substituted complex is that the shorter lifetime of its excited state requires higher quenching constants to produce similar quantum yields of Co(II). The net result is that the calculated maximum quantum yields of Co(II) for the two sensitizers are similar. However, the considerably increased energy transfer and/or poor cage-escape yields for $[Ru^*(4,4'\text{-}Me_2bpy)_3]^{2+}$ resulted in much smaller hydrogen-production rates with this sensitizer. In addition, the substituted ruthenium complex decomposes more rapidly than $[Ru(bpy)_3]^{2+}$. Other alkyl derivatives of $[Ru(bpy)_3]^{2+}$ behave similarly.[69]

Rhodium(III) cage complexes may produce hydrogen spontaneously when reduced to their Rh(II) analogues.[54] Moreover, they do not absorb light in the visible region and therefore do not suffer the internal filtering problems experienced with Co(III). However, in hydrogen-production experiments using $[Rh(diAMsarH_2)]^{5+}$ as an ETA, no hydrogen was detected with or without Pt(PVA) as a catalyst, for both sensitizers. This finding is related to the very negative Rh(III)/Rh(II) redox potentials.[54] The lack of quenching of the $[Ru^*(bpy)_3]^{2+}$ by the rhodium cage complexes is also consistent with the higher energies of the rhodium(III) triplet states compared to those of their cobalt(III) analogues.

Although the cage complexes are more stable than the viologens[49] under the reaction conditions, sacrificial systems containing cage complexes run down more rapidly. Medium changes accompanying the photolysis are a likely contributing factor, since the systems decayed more rapidly after about 1 mol of electrons/mol of edta donor had been supplied. Any reduction in ion association would move the Co(III)/Co(II) couples to more positive potentials.[67] This should have a significant affect on systems utilizing $[Co(CLsar)]^{3+}$ and $[Co(sep)]^{3+}$, which have redox potentials close to that of the hydrogen electrode at pH 5. The viologens have more negative redox potentials and, hence, are not as greatly affected by such changes. Thus, the production of hydrogen, especially with these cage complexes, becomes very sensitive to changes in edta concentration and in pH as the reaction proceeds. However, neither of these factors could impede nonsacrificial water-splitting cycles, which should operate at constant pH.

Finally, coagulation of the catalyst appears to be another cause of faster decay of the photosystem containing the cage complex rather than those containing $mv^{2+}$. It appears that at Pt(PVA) concentrations up to 1 order of magnitude lower than $5 \times 10^{-5}$ M (the most efficient concentration for $mv^{2+}$) the rate of maximum $H_2$ production remains independent of Pt(PVA) concentration. This efficiency in the production of hydrogen must be related to the fast reaction of Pt(PVA) with Co(II). However, the fact that the systems are much shorter lived at the lower platinum concentrations indicates that the lifetime of the catalyst roughly depends on the amount of hydrogen produced per mole of catalyst. This is supported by the lack of coagulation of the catalyst in the absence of hydrogen. These aspects are currently being investigated in more detail.[70]

In summary, the cage complexes have the following advantages over viologens in the photoreduction of water: (i) greater stability of the reduced form of the couple; (ii) photochemical stability of both oxidation states; (iii) stability toward hydrogenation and hydrogenolysis reactions; (iv) cage-escape yields near unity, at least for $[Ru(bpy)_3]^{2+}$; (v) much lower concentrations of platinum catalyst required to give the same rate of hydrogen production. Their disadvantages include the following: (i) slower electron-transfer and competing energy-transfer rates, which require higher concentrations of cage complexes to be used for equivalent hy-

---

(68) Furlong, D. N.; Launikonis, A.; Sasse, W. H. F.; Sanders, J. V. *J. Chem. Soc., Faraday Trans. 1* **1984**, *80*, 571.

(69) Launikonis, A.; Lay, P. A.; Sargeson, A. M.; Sasse, W. H. F., manuscript in preparation.

(70) Furlong, D. N.; Lay, P. A.; Sasse, W. H. F., work in progress.

drogen production; (ii) the absorption of visible light by the Co(III) complexes filtering light in the region of maximum absorption of the sensitizer; (iii) shorter lived sacrificial cycles.

Overall, this work has indicated that the advantages of the cage complexes seem to lie in their larger turnover numbers. There are numerous prospects for increasing their inherent electron-transfer rate constants through the use of either unsaturated derivatives of cage complexes or cage complexes having different donor atoms or alternative polycyclic topologies. These aspects are at present being explored.

**Acknowledgment.** P.A.L. gratefully acknowledges the award of a CSIRO postdoctoral fellowship. We are also grateful for support from a CSIRO/ANU Collaborative Research Grant. We also thank D. Wells for HPLC experiments and Dr. N. Sutin for communication of results prior to publication.

**Registry No.** $[Co(HYMEoxosar\text{-}H)]^{2+}$, 85664-20-6; $[Co(CMMEabsar)]^{3+}$, 85680-90-6; $[Co(EFMEoxosar\text{-}H)]^{2+}$, 85664-18-2; $[Co(sar)]^{3+}$, 85664-13-7; $[Co(AZAMEsar)]^{3+}$, 85664-08-0; $[Co(AMMEsar)]^{3+}$, 85663-97-4; $[Co(diAZAchar)]^{3+}$, 96930-84-6; $[Co(CLsar)]^{3+}$, 85663-92-9; $[Co(sep)]^{3+}$, 72496-77-6; $[Co(MENOsar)]^{3+}$, 85663-83-8; $[Co(CLHOsar)]^{3+}$, 96930-85-7; $[Co(diCLsar)]^{3+}$, 85663-90-7; $[Co(diAMsar)]^{3+}$, 85663-96-3; $[Co(diAMchar)]^{3+}$, 96997-84-1; $[Co(CLNOsar)]^{3+}$, 85663-78-1; $[Co(diNOsar)]^{3+}$, 85663-77-0; $[Co(AZAcapten)]^{3+}$, 81570-78-7; $[Co(AMcapten)]^{3+}$, 92490-34-1; $[Ru(bpy)_3]^{2+}$, 15158-62-0; $[Ru(4,4'\text{-}Me_2bpy)_3]^{2+}$, 32881-03-1; $H_2O$, 7732-18-5; $H_2$, 1333-74-0; Pt, 7440-06-4; methylviologen(2+), 4685-14-7; benzylviologen(2+), 13096-46-3.

---

Contribution from the Department of Chemistry,
University of Iowa, Iowa City, Iowa 52242

# Crystal and Molecular Structures of the Copper(II) and Copper(III) Dithiooxalate Complexes $(18\text{-crown-}6)_2K_2Cu(S_2C_2O_2)_2$ and $([(C_6H_5)_3P]_2N)Cu(S_2C_2O_2)_2$

M. G. KANATZIDIS, N. C. BAENZIGER, and D. COUCOUVANIS*[1]

*Received May 9, 1984*

The crystal and molecular structures of $(18\text{-crown-}6)_2K_2Cu(Dto)_2\cdot DMF$ (I) and $[(Ph_3P)_2N][Cu(Dto)_2]$ (II) are reported. I crystallizes in the monoclinic space group $P2_1/c$ with two molecules per unit cell. The cell dimensions are $a = 11.488$ (2) Å, $b = 8.543$ (2) Å, $c = 23.527$ (7) Å, and $\beta = 93.71$ (2)°. II crystallizes in the monoclinic space group $C2/c$ with four molecules in the unit cell. The cell dimensions are $a = 13.528$ (2) Å, $b = 18.456$ (2) Å, $c = 15.354$ (2) Å, and $\beta = 95.82$ (1)°. Intensity data for both I and II were collected with a four-circle computer-controlled diffractometer with the use of the $\theta$–$2\theta$ step scan technique. The non-hydrogen atoms in I and II were refined with anisotropic temperature factors. Refinement by full-matrix least-squares techniques of 352 parameters on 2783 data for I and of 244 parameters on 2547 data for II gave final $R$ values of 0.06 and 0.05 for I and II, respectively. The hydrogen atoms in I and II were included in the structure factor calculations but were not refined. In I the two independent $Cu^{II}$–S bond lengths in the planar $[Cu(Dto)_2]^{2-}$ anion are 2.254 (2) and 2.268 (2) Å, and the C–C bond length of the Dto ligand is 1.547 (7) Å. The $(18\text{-crown-}6)K^+$ cations are bound to the $\alpha$-diketone portion of the coordinated Dto ligand and weakly interact with the oxygen atom of a DMF molecule of crystallization. The $\overline{K{-}O}$ distance within the crown ether is 2.91 (8) Å, and the K–O(Dto) distance is 2.78 (2) Å. In II the $Cu^{III}$–S bond lengths within the $[Cu(Dto)_2]^-$ anion are 2.164 (1) and 2.178 (1) Å. The C–C bond length of the Dto ligand in II, which readily undergoes photolytic cleavage, is 1.524 (7) Å.

## Introduction

Recently we reported[2] in detail on the rates of the facile oxidation of the $[Cu(Dto)_2]^{2-}$ anion (Dto = $(C_2O_2S_2)^{2-}$, dithiooxalate) with such oxidants as Cu(II) and Fe(III). The $[Cu(Dto)_2]^-$ oxidation product undergoes a light-activated, intramolecular Dto → $Cu^{III}$ electron transfer with cleavage of the C–C bond in the $Dto^{2-}$ ligand[2] and generation of gaseous SCO. The same intramolecular electron transfer also is promoted by triphenylphosphine in the presence or absence of light and results in the cleavage of the C–C bond. The crystal and molecular structures of the $(18\text{-crown-}6)_2K_2Cu(Dto)_2\cdot DMF$ (I) and $[(Ph_3P)_2N]Cu(Dto)_2$ (II) complexes reported in this paper were carried out primarily to determine the C–C bond lengths in the coordinated Dto ligands and the exact coordination geometries around the copper ions in I and II.

## Experimental Section

**Synthesis.** The syntheses of I and II have been reported in detail previously.[2]

**X-ray Diffraction Measurements. Collection and Reduction of Data.** Specific details concerning crystal characteristics and X-ray diffraction methodology for $(KC_{12}H_{24}O_6)_2Cu(Dto)_2\cdot DMF$ and $(PPN)Cu(Dto)_2$ (PPN = bis(triphenylphosphine)nitrogen(1+)) are shown in Table I. A green crystal of I with well-developed faces was selected from a batch of crystals obtained by vapor diffusion of diethyl ether into a DMF solution of the former complex. Red prisms of $(PNP)Cu(Dto)_2$ were obtained by the slow diffusion of pentane into a solution of this complex in $CH_2Cl_2$.

Intensity data for the $[Cu(Dto)_2]^{2-}$ salt were obtained on a Nicolet P3/F four-circle diffractometer automated by a Data General Nova 3 computer with 32K (16 bit words) of memory, a Data General disk unit, and a nine-track tape. The diffractometer was equipped with a molybdenum target X-ray tube ($\lambda$(Mo K$\alpha_1$), 0.709 30 Å) and a graphite crystal monochromator ($2\theta_{max}$ = 12.20°) mounted with equatorial geometry. The lattice constants were determined from the least-squares refinement of $2\theta$, $\omega$, $\phi$, and $\chi$ diffractometer angles of 25 carefully centered reflections with $2\theta$ values between 25 and 40°. Intensity data were collected by a $\theta$(crystal)–$2\theta$(counter) scan in 96 steps using a bisecting geometry. The scan was from $[2\theta(\mathrm{MoK}\alpha_1) - 1.0]°$ to $[2\theta(\mathrm{MoK}\alpha_2) + 1.0]°$. The scan speed was variable from 3.92 to 29.3°/min, depending on the intensity of the reflection. The stability of the crystal was monitored by measuring 3 strong reflections every 80 reflections. No significant changes were observed over the data collection period. Intensity data for the $(PPN)Cu(Dto)_2$ complex were obtained from a crystal lodged in a capillary, which was coated with black enamel paint. A Picker-Nuclear four-circle diffractometer was used. The description of the instrument and the protocol for data acquisition have been described previously.[3] The raw data for both structures were reduced to net intensities, Lorentz–polarization corrections were applied, and the equivalent reflections were averaged.[4] The scattering factors of the neutral nonhydrogen atoms

---

(1) Present address: Department of Chemistry, University of Michigan, Ann Arbor, MI 48109.

(2) Imamura, T.; Ryan, M.; Gordon, G.; Coucouvanis, D. *J. Am. Chem. Soc.* **1984**, *106*, 984. Dto = $C_2O_2S_2^{2-}$ ligand.

(3) Coucouvanis, D.; Kanatzidis, M.; Simhon, E.; Baenziger, N. C. *J. Am. Chem. Soc.* **1982**, *104*, 1874.

0020-1669/85/1324-2680$01.50/0